SCIENTIFIC REPORTS

OPEN

SUBJECT AREAS:
SYNAPTIC TRANSMISSION
GENERAL PHYSICS
STATISTICAL PHYSICS, THERMODYNAMICS AND NONLINEAR DYNAMICS
MODELLING

Received
22 May 2012

Accepted
8 June 2012

Published
2 July 2012

Correspondence and requests for materials should be addressed to J.T. (teramae@riken.jp) or T.F. (tfukai@brain.riken.jp).

Optimal spike-based communication in excitable networks with strong-sparse and weak-dense links

Jun-nosuke Teramae[1,4], Yasuhiro Tsubo[1] & Tomoki Fukai[1,2,3]

[1]RIKEN Brain Science Institute, 2-1 Hirosawa, Wako, Saitama 351-0198, Japan, [2]Brain and Neural Systems Team, RIKEN Computational Science Research Program, 2-1 Hirosawa, Wako, Saitama, 351-0198, Japan, [3]CREST, JST, 4-1-8 Honcho, Kawaguchi, Saitama 332-0012, Japan, [4]PRESTO, JST, 4-1-8 Honcho, Kawaguchi, Saitama 332-0012, Japan.

The connectivity of complex networks and functional implications has been attracting much interest in many physical, biological and social systems. However, the significance of the weight distributions of network links remains largely unknown except for uniformly- or Gaussian-weighted links. Here, we show analytically and numerically, that recurrent neural networks can robustly generate internal noise optimal for spike transmission between neurons with the help of a long-tailed distribution in the weights of recurrent connections. The structure of spontaneous activity in such networks involves weak-dense connections that redistribute excitatory activity over the network as noise sources to optimally enhance the responses of individual neurons to input at sparse-strong connections, thus opening multiple signal transmission pathways. Electrophysiological experiments confirm the importance of a highly broad connectivity spectrum supported by the model. Our results identify a simple network mechanism for internal noise generation by highly inhomogeneous connection strengths supporting both stability and optimal communication.

The dynamics of a complex network depend crucially on the particular connection architecture of the network[1–5]. In the absence of sensory stimulation, cortical networks are far from silent, but generate rich and ubiquitous forms of electrical activity that represent noisy internal brain states. Such states typically display low-frequency (<10 Hz, typically 1–2 Hz) irregular neuronal firing[6–9], interact bidirectionally with sensory experience[10–15], and, moreover, involve a rich repertoire of complex sequential activity patterns[16,17]. There has been much recent interest in the genesis[18–24] and function[10–13] of spontaneous activity or noise in the brain, since noise may be the basic mechanism underlying our percept and decision process, which are essentially probabilistic[14,15]. While the role of network connectivity in complex neural dynamics has been studied extensively[4,25–28], weighted networks have been investigated only recently[29–32] and the dynamical and functional implications of the distribution of link weights remain largely unknown in excitable systems.

Recent experiments revealed that the amplitude of excitatory synaptic potentials (EPSPs) between cortical pyramidal neurons obeys a long-tailed, typically lognormal, distribution[33,34]. Such a distribution creates a synaptic spectrum spanning from vast numbers of weak synapses (typically, the amplitude of EPSP < 1 mV) to a small fraction of extremely strong synapses, for which EPSP amplitude can be several millivolts. Here, we numerically and analytically study the significance of these strong-spare and weak-dense (SSWD) connections for the dynamics of recurrent networks, in which the weights of recurrent excitatory synaptic inputs to each neuron obey a long-tailed distribution. We asked whether reverberating synaptic input generated by such a distribution is sufficient for the genesis of stable spontaneous activity, and whether this internal noise provides an optimal solution for efficient information processing.

Results

The dynamics of each neuron are described by a leaky integrate-and-fire model:

$$\frac{dv}{dt} = -\frac{1}{\tau_m}(v - V_L) - g_E(v - V_E) - g_I(v - V_L), \quad (1)$$

where v is the membrane potential. The membrane time constant τ_m is 20 [ms] for excitatory neurons and 10 [ms] for inhibitory neurons, and the reversal potentials of leak, excitatory and inhibitory postsynaptic currents are

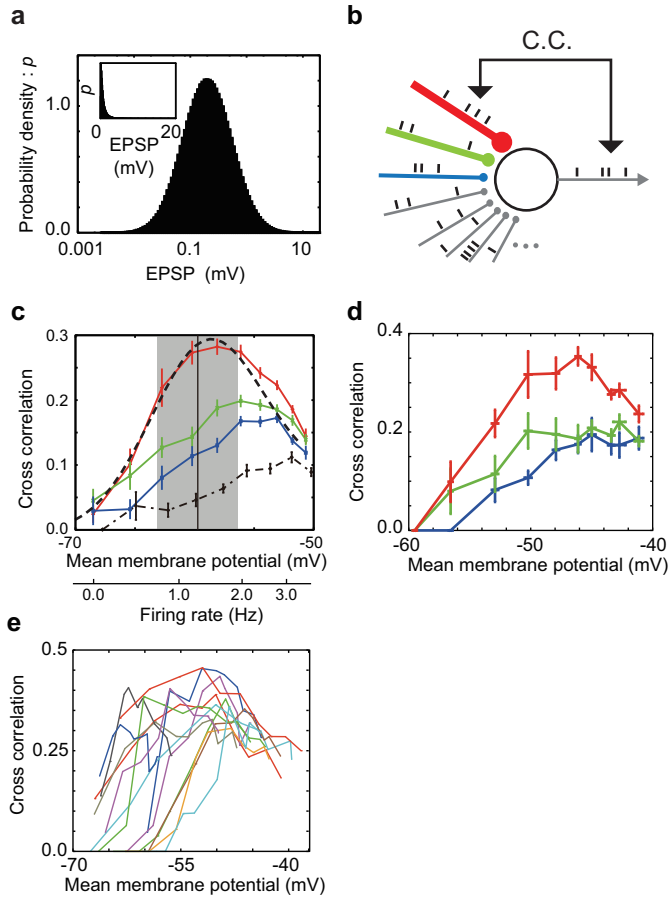

Figure 1 | Maximizing the fidelity of spike transmission with long-tailed sparse connectivity. (a) Each excitatory neuron has a lognormal amplitude distribution of EPSPs. The resultant mean and variance of the model are 0.89 [mV] and 1.1^2 [mV^2], respectively, whereas those shown in a previous experiment [1] were 0.77 [mV] and 0.9^2 [mV^2]. Inset is a normal plot of the same distribution. (b) Schematic illustration of the neuron model with strong-sparse and weak-dense synaptic inputs. Colors (red, green and blue) indicate inputs to the top three strongest weights. (c) C.C.s between the output spike train and input spike trains at the 1st (red), 2nd (green) and 3rd (blue) strongest synapses on a neuron are plotted against the mean membrane potential and the corresponding input firing rate at each synapse. The dashed line and shaded area show the mean and SD of the membrane potential distribution of excitatory neurons shown in Fig. 2f for the SSWD network. Vertical bars represent SEM over different realizations of random input. The dashed line indicates an analytical curve for the strongest synapse of the long-tailed distribution, while the dot-dashed line is the C.C.s for the strongest synapse when EPSP amplitudes obey Gaussian distribution. (d) Similar C.C.s obtained by dynamic clamp recordings from a cortical neuron. The color code and vertical bars are the same as in C. (e) The trial-averaged C.C.s for the strongest synapses on n=14 neurons.

$V_L = -70$ [mV], $V_E = 0$ [mV], $V_I = -80$ [mV], respectively. The excitatory and inhibitory synaptic conductances g_E and g_I [ms^{-1}] normalized by the membrane capacitance obey

$$\frac{dg_X}{dt} = -\frac{g_X}{\tau_s} + \sum_j G_{X,j} \sum_{s_j} \delta(t - s_j - d_j), \quad X = \mathrm{E,I} \qquad (2)$$

where $\delta(t)$ is the delta function, G_j, d_j, s_j are the weight, delay and spike timing of synaptic input from the j-th neuron, respectively. The decay constant τ_s is 2 [ms] and synaptic delays are chosen randomly between $d_0 - 1$ to $d_0 + 1$ [ms], where $d_0 = 2$ for excitatory-to-excitatory connections and $d_0 = 1$ for other connection types. The values are determined from the stability of spontaneous activity (Methods). Spike threshold is $V_{thr} = -50$ [mV] and v is reset to $V_r = -60$ mV after spiking. The refractory period is 1 [ms].

The values of G_i for excitatory-to-excitatory connections are distributed such that the amplitude of EPSPs x measured from the resting potential obey a lognormal distribution

$$p(x) = \frac{\exp\left[-(\log x - \mu)^2 / 2\sigma^2\right]}{\sqrt{2\pi}\sigma x} \qquad (3)$$

on each neuron (Fig. 1a), where the values $\sigma = 1.0$ and $\mu\text{-}\sigma^2 = \log(0.2)$ well replicate the experimentally observed long-tailed distributions of EPSP amplitudes[33,34]. We declined any unrealistic value of G_i that gives an amplitude larger than 20 [mV] by drawing a new value from the distribution. The resultant amplitude of strongest EPSP was about 10 [mV] on each neuron. For simplicity, excitatory-to-inhibitory, inhibitory-to-excitatory and inhibitory-to-inhibitory synapses have uniform values of $G_i = 0.018$, 0.002 and 0.0025, respectively. Excitatory-to-excitatory synaptic transmissions fail at an EPSP amplitude-dependent rate of $p_E = a/(a + \mathrm{EPSP})$, where $a = 0.1$ [mV][34].

We first demonstrate numerically that the long-tailed distribution of EPSP amplitudes achieves aperiodic stochastic resonance for spike sequence on a single neuron receiving random synaptic inputs (Fig. 1b). Stochastic resonance refers to a phenomenon wherein a specific level of noise enhances the response of a nonlinear system to a weak periodic or aperiodic stimulus[35–37], and has been observed in many physical and biological systems[38–45]. We vary the average membrane potential of the neuron by changing the rate of presynaptic spikes at a portion of the weakest excitatory synapses (EPSP amplitudes < 3 mV). Interestingly, the cross-correlation coefficients (C.C.) between output spikes and inputs to the strongest synapses are maximized at a subthreshold membrane potential value about 10 [mV] above the resting potential and 10 [mV] below firing threshold (Fig. 1c). At more hyperpolarized levels of the average membrane potential, even an extremely strong EPSP ($\sim$10 mV) cannot evoke a postsynaptic spike, and the fidelity of spike transmission is reduced. On the contrary at more depolarized average membrane potentials, the neuron can fire without strong inputs, also degrading the fidelity.

We can express the C.C.s in terms of the conditional probability of spiking by strong-sparse input, which we can analytically obtain from the stochastic differential equations for weak-dense synapses (Methods). The analytic results well explain the optimal neuronal response obtained numerically (Fig. 1c). The phenomena can be regarded as stochastic resonance for aperiodic spike inputs[36,37]. We find that the stochastic enhancement of spike transmission is much weaker in a neuron (Fig. 1c, dashed curve) having Gaussian-distributed EPSP amplitude, which give the same mean and variance of synaptic conductances as the lognormal distribution but no tails of strong synapses (Supplementary Methods). The results prove the advantage of long-tailed distributions of EPSP amplitude.

We confirmed the above model's prediction by performing dynamic clamp recordings from cortical neurons (n=14). To mimic synaptic bombardment with long-tailed distributed EPSP amplitudes, we injected the synaptic current given in equation (2) by using the same values of excitatory and inhibitory conductances as used in Fig. 1c (Supplementary Methods). The rate of random synaptic inputs was varied in a low-frequency regime. The physiological result also demonstrated the maximization of the fidelity of synaptic transmission (Fig. 1d, e).

Now, we ask whether the above stochastic resonance is achievable by the noise generated internally by SSWD recurrent neural networks. To see this, we conduct numerical simulations of equations (1) and (2) for a network model of 10000 excitatory and 2000 inhibitory neurons that are randomly connected with coupling probabilities of excitatory and inhibitory connections being 0.1 and 0.5, respectively. Since the network has a trivial stable state in which all neurons are in the resting potentials, we briefly apply external

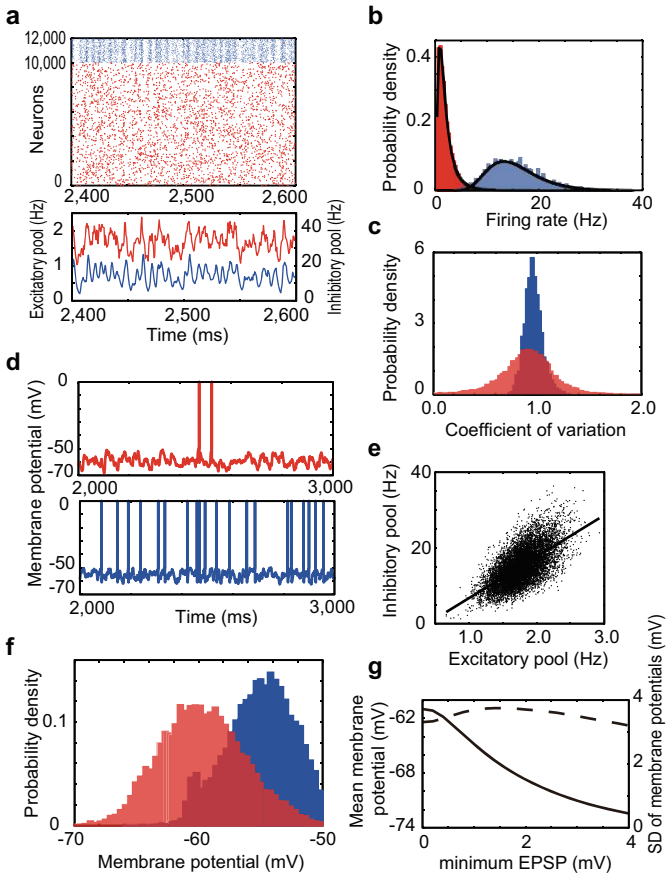

Figure 2 | Spontaneous noise in the SSWD recurrent network. The network receives neither external input nor background noise, and hence activity is spontaneous. (a) *Upper*, Spike raster of excitatory (red) and inhibitory (blue) neurons in the noisy spontaneous firing state. *Lower*, The population firing rates of excitatory (red) and inhibitory (blue) neurons. (b) Firing rate distributions of excitatory (red) and inhibitory (blue) neurons can be fitted by lognormal distributions (black lines). Mean firing rates are 1.6 and 14 [Hz] for excitatory and inhibitory neurons respectively. (c) CVs of inter-spike intervals are distributed around unity in excitatory (red) and inhibitory (blue) neurons. (d) Time courses of the membrane potentials of excitatory (red) and inhibitory (blue) neurons exhibit large amplitude fluctuations. (e) Scatter plot of the instantaneous population activities of excitatory and inhibitory neurons. The solid line represents linear regression. (f) Distribution functions of the fluctuating membrane potentials show the depolarized states of excitatory (red) and inhibitory (blue) neurons. (g) The mean (solid) and standard deviation (dashed) of the membrane potential fluctuations of an excitatory neuron when all EPSPs smaller than the minimum value given in the abscissa are eliminated. Here, we remove a portion of excitatory synapses on a neuron from the weakest ones.

Poisson spike trains to all neurons during initial 100 [ms] to trigger a spontaneous firing. In the absence of external input, the model sustains a stable asynchronous firing initiated by a brief external stimulus (Fig. 2a). The spontaneous network activity emerges purely from reverberating synaptic input, is stable in a very low-frequency regime (Fig. 2b) and is highly irregular (Fig. 2c) as experimentally observed[6,8,9]. Firing rate distributions are well fitted by lognormal distributions[7,46,47]. Each neuron exhibits large membrane potential fluctuations, on top of which spikes are generated occasionally (Fig. 2d), owing to the dynamic balance between excitatory and inhibitory activities (Fig. 2a and 2e)[18,20,24,48]. All these properties are consistent with the spontaneous activity observed in cortical neurons[20]. Importantly, the average values of the membrane potentials are around –60 mV in excitatory neurons (Fig. 2f)[20,49], at which spike transmission at strong-sparse synapses becomes most reliable (Fig. 1a, shaded area). Inputs to weak-dense synapses maintain the average membrane potential of each neuron (Fig. 2g), whereas inputs to strong-sparse synapses govern sparse spiking. Therefore, weak-dense and strong-sparse synapses have different roles in stochastic neural dynamics, although they distribute continuously.

Long-tailed distributions of coupling strengths offer a much wider region of the parameter space to stable spontaneous activity than Gaussian-distributed coupling strengths (Supplementary Fig. 1). Furthermore, a linear stability analysis reveals the homeostasis of the ongoing state of the SSWD network (Methods).

What is the underlying mechanism and functional implications of the spontaneous noise generation? Strong-sparse synapses form multiple synaptic pathways in the recurrent neural network (Fig. 3a). Owing to the stochastic resonance effect at these synapses, spike sequences are routed reliably along these pathways (Fig. 3b: Supplementary Methods) that may branch and converge (Fig. 3c). Since strong synapses are rare, spike propagation along a pathway is essentially unidirectional, as indicated by the cross-correlograms for presynaptic and postsynaptic neuron pairs (Fig. 3d). If, therefore, external stimuli elicit spikes from the initial neurons of some strong pathways, the spikes can stably travel along these pathways without much interference (Fig. 3e). The number of spikes received at the end of a pathway is proportional to that of spikes evoked at the start, although fluctuations in the spike number increase with the distance of travel (Fig. 3f). These results imply that spikes can carry rate information along the multiple synaptic pathways embedded by strong-sparse synapses. The presence of precise spike sequences has been reported in the brain of behaving animals[50–52]. We note that the same spikes are sensed as noise if they are input to weak synapses.

Discussion

In this study, we have explored a coordinating principle in neural circuit function based on a long-tailed distribution of connection weights in a model neural network. The network properties conferred by the long-tailed EPSP distribution account for a role of noise in information routing and present a novel hypothesis for neural network information processing. Namely, we have demonstrated that a single neuron shows spike-based aperiodic stochastic resonance; the cross-correlation coefficient between output spikes of a single neuron and inputs to the strongest synapses are maximized when the neuron receives a certain amount of background noise. Stochastic resonance has been studied in neuronal systems in various contexts. The presence of sensory noise improved behavioral performance in humans[38,41] and other animals[39]. Synaptic bombardment enhanced the responsiveness of neurons to periodic subthreshold stimuli[20,40,42]. Asynchronous neurotransmitter release can give a noise source for stochastic resonance in local circuits of model neurons with short-term synaptic plasticity[43,44]. A surprising result here is that the networks may internally generate optimal noise without external noise sources for the spike-based stochastic resonance on sparse-strong connections. Weak-dense connections redistribute excitatory activity routed reliably on strong connections over the network as optimal noise sources to sustain spontaneous firing of recurrent networks.

Internal noise or asynchronous irregular firing may provide the neural substrate for probabilistic computations by the brain, and how such activity emerges in cortical circuits has been a fundamental problem in cortical neurobiology. Such neuronal firing has been replicated by sparsely connected networks of binary or spiking neurons[18,19,21–23], and the importance of excitation-inhibition balance has been repeatedly emphasized. However, the mechanism to generate extremely low-rate spontaneous asynchronous firing ($\ll$10 Hz) remained unclear, and our model gives a possible solution

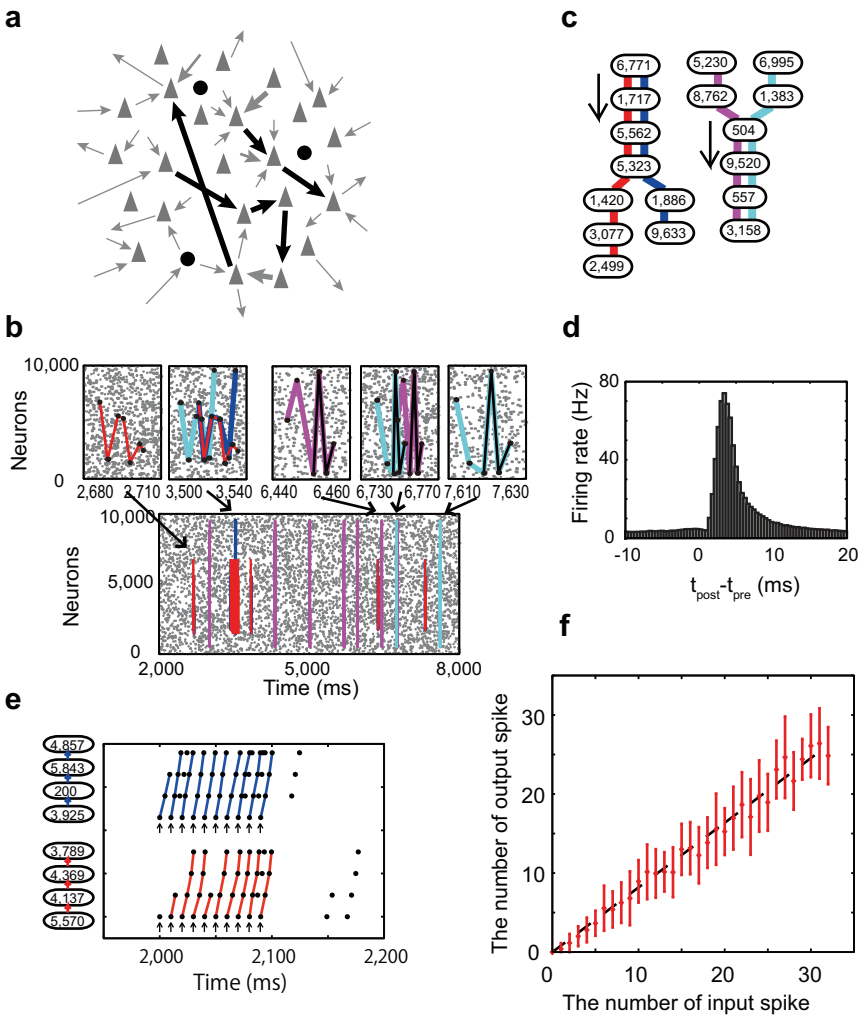

Figure 3 | Spike information routing in the SSWD recurrent network model. (a) A schematic illustration of the SSWD recurrent network. Thick lines stand for strong-sparse connections and thinner lines for weak-dense connections. In reality, the strength of connections is continuous obeying a long-tailed distribution. (b) Examples of spike sequences routed in the network are shown by different colors. Insets magnify the raster plot. (c) Examples of branching (left) and converging (right) pathways formed by the strong synapses. Numbers refer to neurons, and colors to the corresponding pathways in (b). (d) Cross-correlograms are averaged over strongly connected neuron pairs (EPSP >8mV). (e) Repeated external stimuli (arrows) evoke simultaneous spike propagations in two pathways. (f) Linear relationship between the number of input spikes and that of output ones in a pathway. The dashed line and vertical bars represent linear regression and SD over trials, respectively.

to this. A large-scale model of mammalian thalamocortical systems consisting of a million neurons with realistic electrophysiological and morphological properties generated asynchronous irregular states[23], implying that interactions between dynamical and anatomical processes significantly contribute to internal noise generation. By contrast, such states appears in our model from a special synaptic connectivity within local cortical circuits. It is worth while noting that the asynchronous irregular firing of our model does not rely on slow synapses like NMDA receptor-mediated ones. Though slow synapses may improve the stability of such states, our model suggests that such a role of slow synapses is subsidiary.

Long-tailed amplitude distributions of EPSPs can arise from activity-dependent synaptic plasticity. In networks of rate neurons with linear response functions, a Hebbian learning rule induces a lognormal weight distribution when the rule of weight increment depends nonlinearly on the weights[53]. In networks of spiking neurons, spike-timing dependent plasticity results in a long-tailed conductance distribution if the weight dependence for long-term depression[54] depends sublinearly on synaptic weights[55]. Activity-dependent plasticity may switch and reroute different pathways of strong synapses due to sensory or motor experiences of animals while total distribution of EPSP amplitude of the network are kept intact. It is intriguing whether the activity-dependent pathway rerouting may provide a mechanism to represent Bayesian priors of sensory experiences in spontaneous cortical activity[15] and habitual motor coordination[56].

In summary, we conjoin two fundamental principles in signal processing and complex phenomena observed in cortical neural networks: stochastic resonance and noisy internal brain states. The key of this link is the coexistence of a spectrum of strong-sparse and weak-dense connections that gives a mechanism by which excitable networks generate and maintain optimal noise level for efficient spike communication. These results have implications for a role of noise in networks with a broad spectrum of coupling strengths, such as the gating of specific signal pathways with the probabilities of pathway selection modulated by the dynamics of internal noise generation.

Methods

Cross-correlation coefficient. We can analytically calculate cross-correlation coefficients by assuming that spike trains are well approximated by a low-rate Poisson process. Then, the cross-correlation coefficient between input and output spike sequences is estimated as

$$cc = \frac{\langle x_{in}(t)x_{out}(t)\rangle - \langle x_{in}(t)\rangle\langle x_{out}(t)\rangle}{\sqrt{\langle x_{in}^2(t)\rangle - \langle x_{in}(t)\rangle^2}\sqrt{\langle x_{out}^2(t)\rangle - \langle x_{out}(t)\rangle^2}} = \frac{\Pr(x_{in}x_{out})T - r_{in}r_{out}T^2}{\sqrt{r_{in}T - (r_{in}T)^2}\sqrt{r_{out}T - (r_{out}T)^2}} \simeq \Pr(x_{out}|x_{in})\sqrt{\frac{r_{in}}{r_{out}}} \quad (4)$$

where r_{in} and r_{out} are firing rate of input and output sequences respectively, T is a short period of time satisfying $r_{in}T \ll 1$ and $r_{out}T \ll 1$, and $\Pr(x_{out}|x_{in})$ is the conditional probability of output spike for given input spike at strong synapses. In numerical simulation, we evaluated $\Pr(x_{out}|x_{in})$ by detecting a post-synaptic spike within the epoch of EPSP rise from the arrival of an input spike.

Analytical solution of the cross-correlation coefficient. We can analytically calculate the firing rate and cross-correlation coefficient of each neuron by dividing excitatory synaptic inputs to the neuron into two parts, one consisting of weak and modestly strong synapses and one consisting of extremely strong synapses. In this approximation, we may treat inputs to the former excitatory synapses and inhibitory synapses by the diffusion approximation[57], in which Poisson spike inputs on (2) are replaced with a white Gaussian noise having the same mean and variance of the Poisson inputs. We then used the effective-time-constant approximation[58] to replace $v - V_E$ and $v - V_I$ with $V_0 - V_E$ and $V_0 - V_I$ to obtain linear stochastic differential equations

$$\begin{cases} \frac{dv}{dt} = -\frac{(v - V_0)}{\tau_e} + \eta \\ \frac{d\eta}{dt} = -\frac{\eta}{\tau_s} + \sigma\xi \end{cases} \quad (5)$$

where $V_0 = (V_L/\tau_m + V_E g_{E0} + V_I g_{I0})\tau_e$ and $\tau_e = 1/(1/\tau_m + g_{E0} + g_{I0})$ are the equilibrium membrane potential and the effective membrane time constant, respectively. The mean excitatory conductance of the first group and mean inhibitory conductance are $g_{E0} = \tau_s \sum_{i \in \text{1st group}} G_i(1 - p_i)r_i$ and $g_{I0} = \tau_s M_I G_I r_I$, respectively, in terms of the firing rate of the i-th excitatory synaptic input r_i, the synaptic transmission failure p_i, firing rate at inhibitory synapses r_I and the number of inhibitory synapses on the neuron M_I. The fluctuation of the total synaptic current η is given as $\sigma^2 = (V_0 - V_E)^2 \sum_{i \in \text{1st group}} G_i^2(1 - p_i)r_i + (V_0 - V_I)^2 M_I G_I^2 R_I$. The stationary probability density of the membrane potential and the output rate are obtained from equation (5) as[59]

$$P(v) = C \exp\left(-\frac{(v - V_0)^2}{\tau_s^2 \tau_e \sigma^2}\right) \begin{cases} \int_{s_1}^{s_2} e^{s^2} ds, \text{ if } v < v_{reset} \\ \int_{s(v)}^{s_2} e^{s^2} ds, \text{ if } v_{reset} < v < v_{thr} \end{cases}, \quad (6)$$

$$r_{out,\omega} = \left(\tau_{ref} + \tau_e\sqrt{\pi}\int_{s_1}^{s_2} e^{s^2}(1 + \text{erf}(s))ds\right)^{-1} \quad (7)$$

up to the first order of $\sqrt{\tau_s/\tau_m}$, where $\text{erf}(x)$ is the error function and $s_1 = (V_{reset} - V_0)/(\tau_s\sqrt{\tau_e}\sigma) + a\sqrt{\tau_s/\tau_e}/2$, $s_2 = (V_{thr} - V_0)/(\tau_s\sqrt{\tau_e}\sigma) + a\sqrt{\tau_s/\tau_e}/2$, $s(v) = (v - V_0)/(\tau_s\sqrt{\tau_e}\sigma)$, $a = \sqrt{2}|\xi(1/2)|$ and ξ is the Riemann zeta function. Normalization constant C is calculated from the $\int_{-\infty}^{V_{thr}} P(v)dv = 1 - \tau_{ref} r_{out,\omega}$.

The contribution of extremely strong excitatory synapses to output firing is approximated as the sum of the conditional firing probabilities over inputs to these synapses. In the effective-time-constant approximation, the effective amplitude of EPSP evoked by i-th synapse is

$$E_{e,i}(v) = \frac{(V_E - v)\tau_s^{\tau_e/(\tau_e - \tau_s)}\tau_e^{-\tau_s/(\tau_e - \tau_s)}}{(V_E - V_L)\tau_s^{\tau_m/(\tau_m - \tau_s)}\tau_m^{-\tau_s/(\tau_m - \tau_s)}}E_i \equiv \frac{(V_E - v)}{(V_E - V_L)}\beta E_i \quad (8)$$

where v is the membrane potential just before the arrival of presynaptic input and E_i is the EPSP amplitude measured from the resting potential. Because the conditional probability of having an output spike given the i-th input is equal to the area of the stationary density function satisfying $v + E_{e,i}(v) \geq v_{\text{thr}}$, the conditional probability is equal to

$$P_i = \int_{\frac{(V_E - V_L)V_{thr} - \beta E_i V_E}{(V_E - V_L) - \beta E_i}}^{V_{thr}} P(v)dv. \quad (9)$$

Then, by summing these contributions, we obtain the firing rate of the neuron as

$$r_{out} = r_{out,w} + \sum_{i \in \text{2nd group}} P_i r_i \equiv r_{out,w} + r_{out,s}. \quad (10)$$

Finally, by substituting P_i of the strongest synapse into $P(x_{out}|x_{in})$ and using equation (10), we obtain an analytical expression of the correlation coefficient given in equation (4). To derive the analytical curve shown in Fig. 1c, we classified the five strongest synapses into the second group and the remaining ones into the first group.

Stability of sparse spontaneous activity. Using the above analytic results, we can derive a coupled evolution equation for the average firing rates of excitatory and inhibitory neuron pools. Since neurons are connected in a non-biased manner, we can use the mean-field approximation.

The firing rates of excitatory and inhibitory neuron pools, r_E and r_I can vary in time due to interactions between them. Since the mean output rate is equal to the mean rate of input given synaptic delays in a recurrent network, we may represent the time evolution of the mean firing rates of these neuron pools as the following relaxation process with their effective membrane time constants:

$$\begin{cases} \frac{dr_E}{dt} = -\frac{1}{\tau_{e,E}}(r_E(t) - r_{out,E}(r_E(t - d_{EE}), r_I(t - d_{EI}))) \\ \frac{dr_I}{dt} = -\frac{1}{\tau_{e,I}}(r_I(t) - r_{out,I}(r_I(t - d_{IE}), r_I(t - d_{II}))) \end{cases}, \quad (11)$$

where $r_{out,E}(r_E, r_I) = r_{out,s} + r_{out,w}$ and $r_{out,I}(r_E, r_I)$ is similar to $r_{out,w}$ if we replace the average excitatory-to-inhibitory and inhibitory-to-inhibitory synaptic conductances with their unique values in equation (7). Constants d_{XY} represent the mean synaptic delays from Y neurons to X neurons (X, Y = E or I). We can obtain the nullclines of r_E and r_I shown in Supplementary Fig. 2 by equating the left-hand sides of equation (11) to zero. Sustained spontaneous activity may correspond to a nonzero intersection (r_{E0}, r_{I0}) of the two nullclines. The stability of spontaneous activity can be studied by the linear stability analysis: we substitute $r_E(t) = r_{E0} + \varepsilon e^{\lambda\tau}$ and $r_I(t) = r_{I0} + \varepsilon c e^{\lambda}$ in equation (11) and expand the equation up to the linear order in ε. Then, the elimination of ε and c from the resultant equation gives a closed-form equation for the stability index λ:[60]

$$\left(\lambda\tau_{e,E} + 1 - a_{EE}e^{-\lambda\tau_{EE}}\right)\left(\lambda\tau_{e,I} + 1 - a_{II}e^{-\lambda\tau_{II}}\right) = a_{IE}e^{-\lambda\tau_{IE}}a_{EI}e^{-\lambda\tau_{EI}}. \quad (12)$$

We solve Equation (12) numerically to obtain the stable region in the parameter space (Supplementary Fig. 2). The results of the theoretical analysis well coincide with those of numerical simulations.

1. Watts, D. J. & Strogatz, S. H. Collective dynamics of "small-world" networks. *Nature* **393**, 440–442 (1998).
2. Argollo de Menezes, M. & Barabási, A. L. Fluctuations in Network Dynamics. *Phys. Rev. Lett.* **92**, 028701 (2004).
3. Bullmore, E. & Sporns, O. Complex brain networks: graph theoretical analysis of structural and functional systems. *Nat. Rev. Neurosci.* **10**, 186–198 (2009).
4. Chialvo, D. R. Emergent complex neural dynamics. *Nature Phys.* **6**, 744–750 (2010).
5. Pajevic, S. & Plenz, D. The organization of strong links in complex networks. *Nature Phys.* **8**, 429–436 (2012).
6. Softky, W. & Koch, C. The highly irregular firing of cortical cells is inconsistent with temporal integration of random EPSPs. *J. Neurosci.* **13**, 334–350 (1993).
7. Hromádka, T., DeWeese, M. R. & Zador, A. M. Sparse representation of sounds in the unanesthetized auditory cortex. *PLoS Biol.* **6**, e16 (2008).
8. Sakata, S. & Sakata, S. & Harris, K. D. Laminar structure of spontaneous and sensory-evoked population activity in auditory cortex. *Neuron* **64**, 404–418 (2009).
9. Mizuseki, K., Diba, K., Pastalkova, E. & Buzsáki, G. Hippocampal CA1 pyramidal cells form functionally distinct sublayers. *Nat. Neurosci.* **14**, 1174–1181 (2011).
10. Katz, L. C. & Shatz, C. J. Synaptic Activity and the Construction of Cortical Circuits. *Science* **274**, 1133–1138 (1996).
11. Kenet, T., Bibitchkov, D., Tsodyks, M. V., Grinvald, A. & Arieli, A. Spontaneously emerging cortical representations of visual attributes. *Nature* **425**, 954–956 (2003).
12. Petersen, C. C., Hahn, T. T. G., Metha, M., Grinvald, A. & Sakmann, B. Interaction of sensory responses with spontaneous depolarization in layer 2/3 barrel cortex. *Proc. Natl. Acad. Sci. USA* **100**, 13638–13643 (2003).
13. MacLean, J., Watson, B., Aaron, G. & Yuste, R. Internal dynamics determine the cortical response to thalamic stimulation. *Neuron* **48**, 811–823 (2005).
14. Luczak, A., Bartho, P. & Harris, K. D. Spontaneous events outline the realm of possible sensory responses in neocortical populations. *Neuron* **63**, 413–425 (2009).
15. Berkes, P., Orbán, G., Lengyel, M. & Fiser, J. Spontaneous cortical activity reveals hallmarks of an optimal internal model of the environment. *Science* **331**, 83–87 (2011).
16. Beggs, J. M. & Plenz, D. Neuronal avalanches in neocortical circuits. *J. Neurosci.* **23**, 11167–11177 (2003).
17. Petermann, T., Thiagarajan, T. C., Lebedev, M. A., Nicolelis, M. A. L., Chialvo, D. R. & Plenz, D. Spontaneous cortical activity in awake monkeys composed of neuronal avalanches. *Proc. Natl. Acad. Sci. USA* **106**, 15921–15926 (2009).
18. van Vreeswijk, C. & Sompolinsky, H. Chaos in neuronal networks with balanced excitatory and inhibitory activity. *Science* **274**, 1724–1726 (1996).
19. Brunel, N. Dynamics of sparsely connected networks of excitatory and inhibitory spiking neurons. *J. Comput. Neurosci.* **8**, 183–208 (2000).
20. Destexhe, A., Rudolph, M. & Paré, D. The high-conductance state of neocortical neurons in vivo. *Nat. Rev. Neurosci.* **4**, 739–751 (2003).
21. Vogels, T. P. & Abbott, L. F. Signal propagation and logic gating in networks of integrate-and-fire neurons. *J. Neurosci.* **25**, 10786–10795 (2005).

22. Kumar, A., Schrader, S., Aertsen, A. & Rotter, S. The high-conductance state of cortical networks. *Neural Comput.* **20**, 1–43 (2008).
23. Izhikevich, E. M., Edelman, G. M. Large-scale model of mammalian thalamocortical systems. *Proc. Natl. Acad. Sci. USA* **105**, 3593–3598 (2008).
24. Renart, A. *et al.* The asynchronous state in cortical circuits. *Science* **327**, 587–590 (2010).
25. Yoshimura, Y. & Callaway, E. M. Fine-scale specificity of cortical networks depends on inhibitory cell type and connectivity. *Nat. Neurosci.* **8**, 1552–1559 (2005).
26. Volman, V. & Perc, M. Fast random rewiring and strong connectivity impair subthreshold signal detection in excitable networks. *New J. Phys.* **12**, 043013 (2010).
27. Sun, X., Lei, J., Perc, M., Kurths, J. & Chen, G. Burst synchronization transitions in a neuronal network of subnetworks. *Chaos* **21**, 016110 (2011).
28. Perin, R., Berger, T. K. & Markram, H. A synaptic organizing principle for cortical neuronal groups. *Proc. Natl. Acad. Sci. USA* **108**, 5419–5424 (2011).
29. Barrat, A., Barthélemy, M., Pastor-Satorras, R. & Vespignani, A. The architecture of complex weighted networks. *Proc. Natl. Acad. Sci. USA* **101**, 3747–3752 (2004).
30. Bianconi, G. Emergence of weight-topology correlations in complex scale-free networks. *Europhys. Lett.* **71**, 1029–1035 (2005).
31. Serrano, M. A., Boguñá, M. & Pastor-Satorras, R. Correlations in weighted networks. *Phys. Rev. E*, **74**, 55101 (2006).
32. Restrepo, J. G., Ott, E. & Hunt, B. R. Weighted percolation on directed networks. *Phys. Rev. Lett.* **100**, 58701 (2008).
33. Song, S., Sjöström, P. J., Reigl, M., Nelson, S. B. & Chklovskii, D. B. Highly nonrandom features of synaptic connectivity in local cortical circuits. *PLoS Biol.* **3**, e68 (2005).
34. Lefort, S., Tomm, C., Floyd Sarria, J. C. & Petersen, C. C. H. The excitatory neuronal network of the C2 barrel column in mouse primary somatosensory cortex. *Neuron* **61**, 301–316 (2009).
35. Wiesenfeld, K. & Moss, F. Stochastic resonance and the benefits of noise: from ice ages to crayfish and SQUIDs. *Nature* **373**, 33–36 (1995).
36. Collins, J. J., Chow, C. C. & Imhoff, T. T. Stochastic resonance without tuning. *Nature* **376**, 236–238 (1995).
37. Collins, J., Chow, C. C., Capela, A. C. & Imhoff, T. T. Aperiodic stochastic resonance. *Phys. Rev. E* **54**, 5575–5584 (1996).
38. Collins, J. J., Imhoff, T. T. & Grigg, P. Noise-enhanced tactile sensation. *Nature* **383**, 770 (1996).
39. Russell, D. F., Wilkens, L. A. & Moss, F. Use of behavioural stochastic resonance by paddle fish for feeding. *Nature* **402**, 291–294 (1999).
40. Rudolph, M. & Destexhe, A. Do neocortical pyramidal neurons display stochastic resonance? *J. Comput. Neurosci.* **11**, 19–42 (2001).
41. Kitajo, K., Nozaki, D., Ward, L. M. & Yamamoto, Y. Behavioral stochastic resonance within the human brain. *Phys. Rev. Lett.* **90**, 218103 (2003).
42. Wolfart, J., Debay, D., Le Masson, G., Destexhe, A. & Bal, T. Synaptic background activity controls spike transfer from thalamus to cortex. *Nat. Neurosci.* **8**, 1760–1767 (2005).
43. Volman, V. & Levine, H. Activity-dependent stochastic resonance in recurrent neuronal networks. *Phys. Rev. E* **77**, 060903 (2008).
44. Volman, V. & Levine, H. Signal processing in local neuronal circuits based on activity-dependent noise and competition. *Chaos* **19**, 033107 (2009).
45. McDonnell, M. D. & Ward, L. M. The benefits of noise in neural systems: bridging theory and experiment. *Nat. Rev. Neurosci.* **12**, 415–426 (2011).
46. Mizuseki, K., Sirota, A., Pastalkova, E. & Buzsáki, G. Theta oscillations provide temporal windows for local circuit computation in the entorhinal-hippocampal loop. *Neuron* **64**, 267–280 (2009).
47. Roxin, A., Brunel, N., Hansel, D., Mongillo, G. & van Vreeswijk, C. On the distribution of firing rates in networks of cortical neurons. *J. Neurosci.* **31**, 16217–16226 (2011).
48. Shu, Y., Hasenstaub, A. & McCormick, D. Turning on and off recurrent balanced cortical activity. *Nature* **423**, 288–293 (2003).
49. Steriade, M., Timofeev, I. & Grenier, F. Natural waking and sleep states: a view from inside neocortical neurons. *J. Neurophysiol.* **85**, 1969–1985 (2001).
50. Abeles, M., Bergman, H., Margalit, E. & Vaadia, E. Spatiotemporal firing patterns in the frontal-cortex of behaving monkeys. *J. Neurophysiol.* **70**, 1629–1638 (1993).
51. Long, M. A., Jin, D. Z. & Fee, M. S. Support for a synaptic chain model of neuronal sequence generation. *Nature* **468**, 394–399 (2010).
52. Hahnloser, R. H., Kozhevnikov, A. A. & Fee, M. S. An ultra-sparse code underlies the generation of neural sequences in a songbird. *Nature* **419**, 65–70 (2002).
53. Koulakov, A., Hromádka, T. & Zador, A. M. Correlated connectivity and the distribution of firing rates in the neocortex. *J. Neurosci.* **29**, 3685–3694 (2009).
54. van Rossum, M. C. W., Bi, G. Q. & Turrigiano, G. G. Stable Hebbian learning from spike timingdependent plasticity. *J. Neurosci.* **20**, 8812–8821 (2000).
55. Gilson, M. & Fukai, T. Stability versus neuronal specialization for STDP: long-tail weight distributions solve the dilemma. *PLoS ONE* **6**, e25339 (2011).
56. de Rugy, A., Loeb, G. E. & Carroll, T. J. Muscle coordination is habitual rather than optimal. *J. Neurosci.* **32**, 7384–7391 (2012).
57. Tuckwell, H. C. *Introduction to Theoretical Neurobiology* (Cambridge Univ. Press, Cambridge, 1998).
58. Burkitt, A. N. A review of the integrate-and-fire neuron model: I. Homogeneous synaptic input. *Biol. Cybern.* **95**, 1–19 (2006).
59. Fourcaud-Trocme, N. & Brunel, N. Dynamics of the firing probability of noisy integrate-and-fire neurons. *Neural Comput.* **14**, 2057–2110 (2002).
60. Roxin, A., Brunel, N. & Hansel, D. Role of delays in shaping spatiotemporal dynamics of neuronal activity in large networks. *Phys. Rev. Lett.* **94**, 238103 (2005).

Acknowledgements

The authors thank K. Harris for valuable comments on an early version of this manuscript. The authors greatly benefited from fruitful discussions with T. Vogels and L.F. Abbott. This work was partially supported by JST CREST and PRESTO programs, KAKENHI 24120524 (to J.T.), 22700323 (to Y.T.) and 22115013 (to T.F.).

Author contributions

J.T. and T.F. designed the study and wrote the manuscript. J.T. performed theoretical and numerical analyses and Y.T. performed experiments.

Additional information

Supplementary information accompanies this paper at http://www.nature.com/scientificreports

Competing financial interests: The authors declare no competing financial interests.

How to cite this article: Teramae, J., Tsubo, Y. & Fukai, T. Optimal spike-based communication in excitable networks with strong-sparse and weak-dense links. *Sci. Rep.* **2**, 485; DOI:10.1038/srep00485 (2012).